

Electrochemical impregnation and performance of nickel hydroxide electrodes with porous plaques of hollow nickel fibres

Wen-Hua Zhu, Deng-Jun Zhang, Jia-Jun Ke

Institute of Chemical Metallurgy, Chinese Academy of Sciences, Beijing 100080, China

Received 2 June 1995; accepted 21 July 1995

Abstract

Porous plaques that contain hollow nickel fibres are successfully prepared by a traditional slurry-scraping technology. The fibrous, nickel-plaque materials have high porosity (85–87%) and are for application in high specific-energy nickel–metal hydride batteries. Nickel electrodes are fabricated by cathodic electrodeposition from metal nitrate solutions on to the fibrous plaques. Parameter changes in the concentration of nickel nitrate, current density, pH, temperature and plaque porosity, as well as changes in the impregnation time, are examined with respect to their influence on the weight gain of fibrous nickel plaques. The influence of fibre content on the electrode performance is investigated by determining the capacity, utilization, expansion and cycling characteristics. Both C-type and D-type electrodes with ~85% fibrous plaques reach a specific capacity of 141 mAh g⁻¹. It is found that utilization of active material and electrode swelling both decrease with increasing content of the hollow fibres.

Keywords: Electrodes; Nickel hydroxide; Nickel fibres

1. Introduction

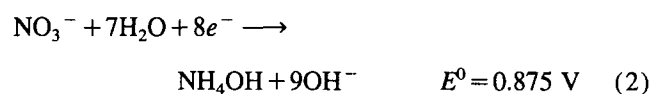
Nickel electrodes of sealed, cylindrical nickel–cadmium and nickel–metal hydride cells depend on the use of thin, flexible, porous nickel plaque. The industrial process for manufacturing new collectors for nickel–cadmium, nickel–hydrogen and nickel–metal hydride batteries with high specific energy has been developed at DAUG, SORAPEC, CNRS, NSW, etc. [1–3]. The foam plaque with its moderate conductivity and large pore size is an effective material for low-to-medium rate applications, but it is poor at high power and has a limited cycle life. The fibre-structured plaque with a unique small pore size and high porosity has been reported [4] to have excellent elasticity. The porous nickel support, Fibrex¹, which can be found in commercial products (fibre and felt, nickel-plated plastic and graphite plaques), has good dimensional stability and active material adherence and over a 3000-cycle life [5]. Highly porous and thick Fibrex plaques are attractive potential candidates for a lightweight nickel–hydrogen cell [6]. The Fibrex plaque is formed by the reduction and sintering of fibres extruded from a mixture of nickel oxide and binder agents [7,8]. Another method of manufacture is based on a chemical or physical plating of organic fibres, followed by nickel electrodeposition [9–11]. The

nickel-coated fibres are then pyrolyzed and sintered under a suitable atmosphere. The authors have also proposed a chemical metallurgy method to produce hollow nickel fibres [12]. The hollow fibres can be used to fabricate the porous plaque and to improve the material porosity and flexibility.

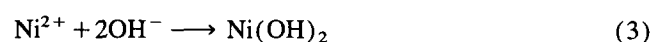
The electrochemical impregnation (ECI) of introducing active material into the porous nickel plaque is a rapid-filling process in preparing the nickel hydroxide electrode [13–15]. Kandler [16] was the first to propose that precipitation within the pores is brought about by a change in pH during NO₃⁻ reduction. The following equation was quantitatively demonstrated by analyzing the NH₄⁺ ions of the impregnation solution [17]:



Takamura et al. [18] conducted the ECI process at higher current densities and found that the amount of NH₄OH is directly proportional to the amount of input charge:



Therefore, hydroxide ions, generated by the reduction of nitrate ions, precipitate the nickel ions to form the active nickel hydroxide in the pores as follows:

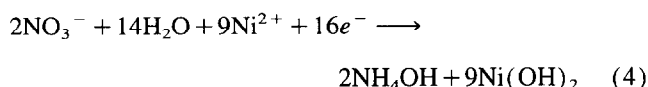


¹ Trademark of National Standard Corporation, MI, USA.

Table 1
Features of porous plaques with hollow nickel fibres and characteristics of electrodes

Type	A	B	C	D	E
Content of fiber (wt.%)	25	50	50	75	100
Plaque porosity (wt.%)	74	78	85	86	87
Loading level (g cm^{-3} void)			2.0	2.0	1.9
Plaque thickness (mm)	0.7	0.9	0.9	1.2	1.2
Theoretical specific capacity (mAh g^{-1})			156	164	162
Actual specific capacity (mAh g^{-1})			141	141	126
Utilization (% , fourth discharge at 0.2C)			90.3	86.5	77.6
Expansion of fourth cycle (%)			11.8	8.5	6.4

The overall reaction at the cathode is expressed as:



Further studies on the cathodic ECI process have been conducted by several authors [19–23]. The impregnation process is probably the most important and complex operation in battery manufacturing. With the conventional chemical method, it is difficult to deposit the active material inside the pores of the plaque without precipitation in the bulk solution and on the outside of the plaque surface. The ECI process mentioned above has received increasing attention in the manufacturing of rechargeable batteries. The technology is a simple process and the precipitation speed and the adherence

of nickel hydroxide are superior to the traditional vacuum impregnation method [24]. A production facility has been set up to manufacture nickel–hydrogen and nickel–cadmium cells by the method [25].

Engineering studies [13,21–23] have also been carried out by many authors, but the ECI process of porous nickel plaque is relatively complex and it is difficult to define optimum process conditions for attaining a moderate loading level. There are many parameters that control the ECI process, namely, concentration of nickel nitrate, current density, temperature of solution, pH, porosity of nickel plaque material, composition of bulk solution, impregnation time, etc.

Mutual parameters that affect the weight gain of sintered fibrous nickel plaques are examined in the work reported here by the one-step ECI process. The performance of fibrous nickel electrodes is also measured in order to understand the electrochemical characteristics.

2. Experimental

2.1. Sintering preparation of porous plaques containing hollow nickel fibres

The porous plaques were formed by coating perforated nickel-plated mild-steel/ or iron strips that were subsequently dried and subjected to a high-temperature reducing atmosphere. The slurry consisted of a mixture of carbonyl nickel powder and hollow nickel fibres with an aqueous solution of carboxymethyl cellulose. The nickel fibres were first prepared on organic non-woven material under a middle temperature, non-oxidizing environment in a pressured reactor, and then pyrolyzed to form the hollow nickel structure. The features of the fibres themselves and different porous plaques prepared by the method are shown in Table 1 and Figs. 1 and 2.

2.2. Electrochemical impregnation of fibrous nickel plaques

The electrochemical impregnation system comprised the following: electrolytic cell, pH meter, current generator, constant-temperature controller, magnetic stirrer, voltmeter. The electrolytic cell consisted of a porous nickel plaque placed between two bulk nickel anodes. The volume of nickel nitrate

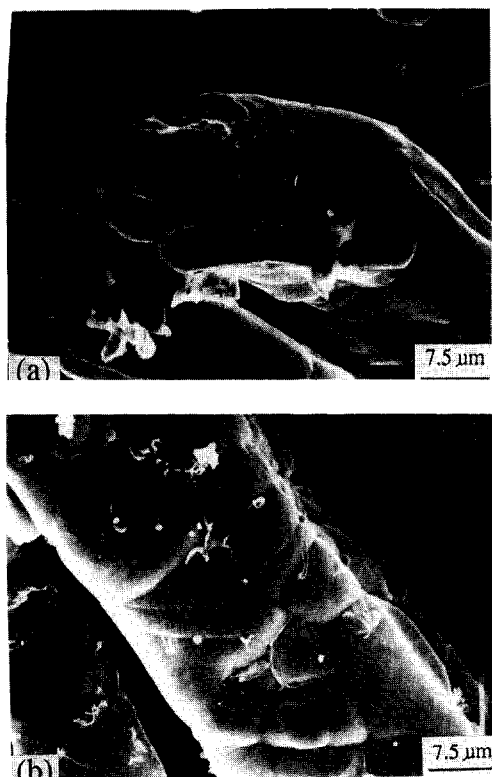


Fig. 1. Electron micrographs of hollow nickel fibres prepared by a chemical metallurgical method: (a) hollow nickel fibre, and (b) growth traces of single fibre.

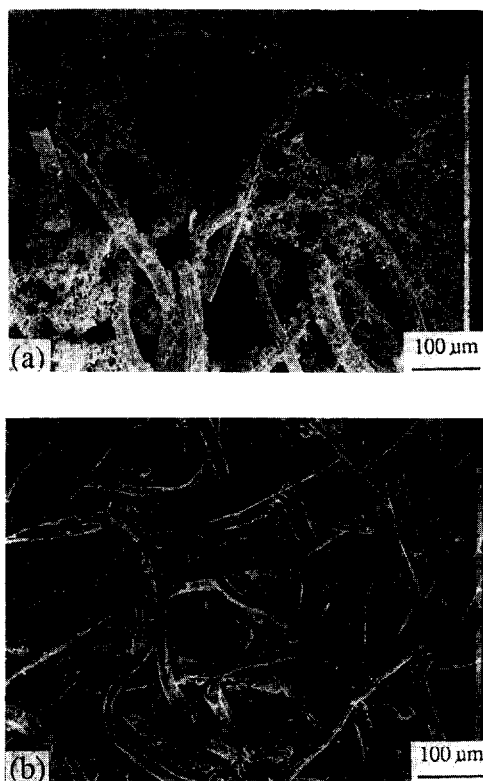


Fig. 2. Electron micrographs of porous nickel plaques: (a) 50% fibrous plaque, and (b) 100% fibrous plaque.

solution was 260 ml. The solution temperature was controlled by a thermostat (± 1 °C) and the concentration of nickel nitrate was determined by measuring the specific gravity with a Baume gravimeter. The pH was adjusted with 4 M HNO_3 or nickel hydroxide.

In general, experiments were conducted at 60 mA cm^{-2} by means of a stabilized current generator. The temperature was varied between 30 and 75 °C. All electrodes were washed with de-ionized water and then immersed in aqueous NaOH solution (density 1.20 g cm^{-3}) at 90 °C for about 30 min, to remove the ammonium hydroxide and other substances inside the pores. The plaques were then removed, washed and dried at 90 °C until they recorded a constant weight. The weight gain was measured by analytical scales. A special ECI process was conducted by filling the porous plaque with high concentrated $\text{Ni}(\text{NO}_3)_2$ ($1.69\text{--}1.71 \text{ g cm}^{-3}$, 100 °C) by means of a vacuum method, and then applying the electrochemical operation.

Three of the nickel electrodes (C-, D- and E-types) were prepared at 90 °C by the ECI method. Additives of 5 wt.% $\text{Co}(\text{NO}_3)_2$ and 5 wt.% $\text{Ca}(\text{NO}_3)_2$ were used in the 2.0 M $\text{Ni}(\text{NO}_3)_2$, 0.10 M NaNO_2 impregnation solution. Dry electrodes were immersed in 26% KOH solution for 5 h before the cycle operation and measurement.

2.3. Cycling and performance tests

Cycling tests were performed on a simple cell with two nickel foil counter electrodes on both sides of the porous

nickel oxide working electrode. A HgO/Hg reference electrode in 6 M KOH had a contact with the working solution through a capillary that was separated from the working electrode by 1 mm. The formation electrodes were charged at a rate of 0.4C to 150% of their theoretical capacity (calculated from deposited active material) and discharged at 0.2C to 0.0 V versus HgO/Hg electrode for three repeated operations. The discharge capacity on the fourth cycle was determined at the 0.2C rate after a charge process at 0.2C for 7.5 h. The cycling tests were carried out at ambient temperature (18 °C) and cells during the fifth to fourteenth cycle operation were charged at the 0.5C rate for 160 min, followed by a discharge at 0.3C to 0.0 V vs. HgO/Hg electrode.

The thickness of each test electrode was measured by means of a micrometer at several predetermined locations. Scanning electron micrographs were obtained by using an HITACHI S-450 electron microscope.

3. Results and discussion

3.1. Microstructure of hollow nickel fibres and porous plaques

Hollow nickel fibres, fabricated by a chemical metallurgy method [12], are shown in Figs. 1 and 2. An unsintered single fibre is presented in Fig. 1(a); the hollow structure can be seen clearly. A higher-magnification micrograph of the fibre is shown in Fig. 1(b); the growth traces of the nickel particles are readily visible. The structures of two fibrous nickel plaques are given in Fig. 2. The micro-welding contacts of nickel particles are produced by a sintering process under a hydrogen reducing atmosphere.

3.2. Effect of electrochemical impregnation parameters on weight gain of fibrous nickel plaques

A one-step electrochemical deposition was performed without any additive. The loading level, ρ_L , is calculated from the following relationship:

$$\rho_L = \frac{w_1 \rho_0}{m_0'} (1/\varphi - 1) \quad (5)$$

where: w_1 , ρ_0 and m_0' refer to the total weight gain, specific gravity of nickel metal and initial weight of the plaques without tabs, respectively; φ is the plaque porosity. The weight gain was used directly to describe the deposition of active material. In Figs. 3 to 8, the thick lines refer to the special ECI process and the thin lines to the conventional process. The same initial concentration of $\text{Ni}(\text{NO}_3)_2$ in the fibrous nickel plaque and the electrolyte are applied in the conventional ECI method. The special ECI process was carried out according to the method given above.

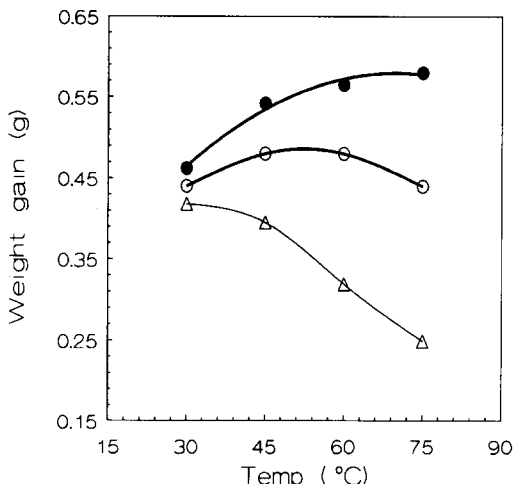


Fig. 3. Effect of temperature on weight gain of porous nickel plaques B-type: (●) 83 min, and (△, ○) 45 min; $[Ni(NO_3)_2] = 3.2 M$; $pH = 3.5 \pm 0.15$.

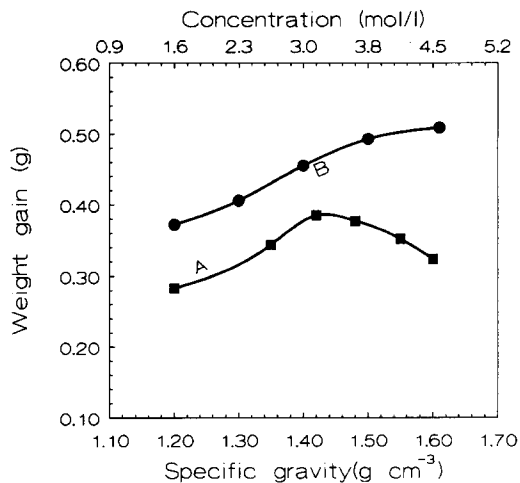


Fig. 4. Effect of changes in electrolyte concentration of nickel nitrate on weight gain of porous nickel plaques. A-type, B-type: $i = 60 mA cm^{-2}$; $pH = 3.5 \pm 0.15$, $60^\circ C$, and 50 min.

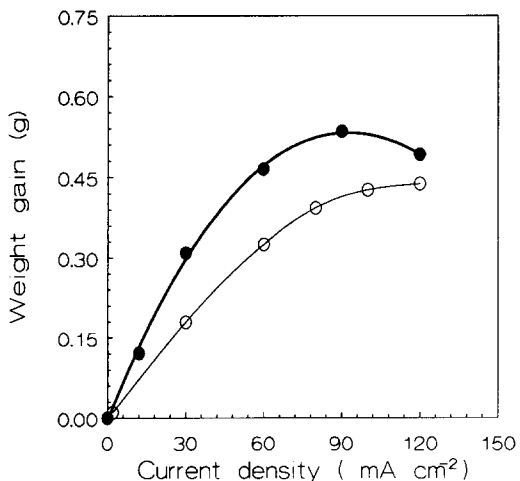


Fig. 5. Weight gain as function of current density. B-type: $[Ni(NO_3)_2] = 3.2 M$; $60^\circ C$; 45 min; $pH = 3.5 \pm 0.15$.

3.2.1. Temperature

Increasing the temperature in 83 min increases the final weight gain of the nickel plaque material for the special ECI process (Fig. 3). The deposition of active material occurs on the surface of the nickel plaque or on the walls of the outer pores at a lower temperature, but in the inner pores at a higher temperature. The last mentioned feature results from the higher solubility of nickel hydroxide in a hot acid solution. After 45 min, the weight gain with the special process was greater than that with the traditional process. The practical current density gradually increases with the reducing surface area of undeposited nickel plaque and this makes it possible to precipitate $Ni(OH)_2$ on the walls of outer pores. High temperature promotes the diffusion and migration of Ni^{2+} and NO_3^- and hence increases the weight gain with the ECI process. On the other hand, high temperature accelerates the anodic corrosion of nickel plates and Ni^{2+} ions have the possibility to form nickel metal on the surface of the cathode

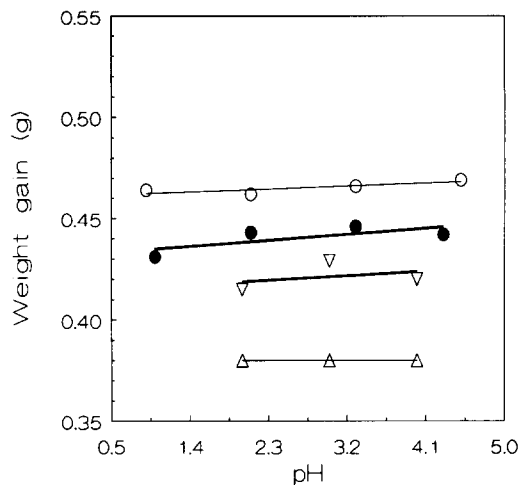


Fig. 6. Effect of pH value on weight gain of porous nickel plaque. B-type: (△, ▽) $60^\circ C$, and (○, ●) $30^\circ C$; $[Ni(NO_3)_2] = 3.2 M$; 45 min.

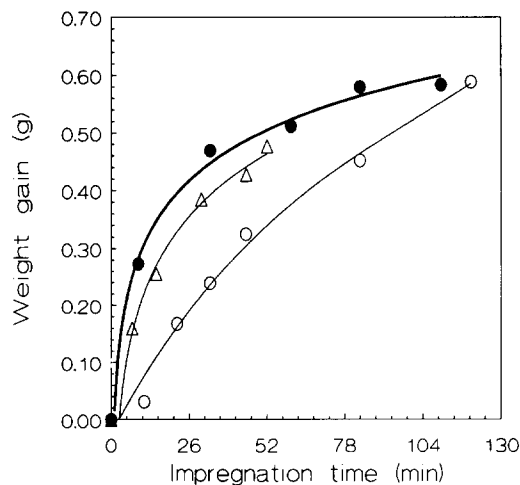


Fig. 7. Weight gain at two different current densities over a period of time. B-type: (△) $100 mA cm^{-2}$, and (●, ○) $60 mA cm^{-2}$; $[Ni(NO_3)_2] = 3.2 M$; $pH = 3.5 \pm 0.15$; $60^\circ C$.

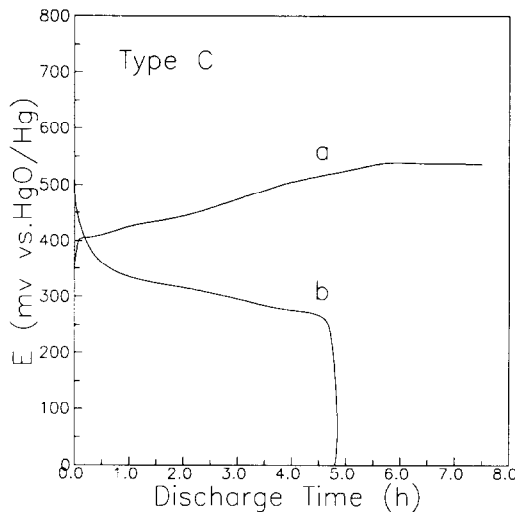


Fig. 8. Curves for (a) fourth charge and (b) fourth discharge for C-type electrode. Charge: $0.2C$ for 7.5 h; discharge: $0.2C$ to 0.0 V vs. HgO/Hg electrode.

plaque. Law and Sapjeta [20] reported that the best capacities were obtained at 70°C and electrode capacities were somewhat lower in the range of $40\text{--}60^{\circ}\text{C}$. By contrast, Ramos et al. [26] successfully conducted the ECI process at 40°C with $4.5\text{ M Ni}(\text{NO}_3)_2$ and using 85% porosity plaques after a mechanical impregnation; a moderate loading level of practical use was obtained. Therefore, lower temperature can also be applied to fill the active material into the porous nickel plaque for industrial operations.

3.2.2. Concentration of nickel nitrate

The filling amounts of nickel hydroxide are dependent upon the concentration of nickel nitrate (Fig. 4). There is an optimal concentration range ($2.8\text{--}3.5\text{ M}$) for the A-type plaque with the special ECI process. The B-type plaque has a higher porosity and a higher concentration ($3.7\text{--}4.4\text{ M}$) and is more suitable in a limited period with the rapid ECI process. It appears that most of the Ni^{2+} ions diffuse into the pores to form nickel hydroxide in the porous plaque. A higher-diffusion flux of Ni^{2+} ions is helpful for the ECI process. The diffusion coefficient of Ni^{2+} ions is lower, but the concentration gradient is higher in the concentrated solution. From Fig. 4, it can be seen that the weight gain of the A-type nickel plaque reaches a maximum value in $3.2\text{ M Ni}(\text{NO}_3)_2$ solution over 50 min and that the B-type is preferred in a more concentrated solution. In general, the overall flux of Ni^{2+} ions depends on both the plaque construction and the operation conditions. The choice of $\text{Ni}(\text{NO}_3)_2$ concentration depends on the nature of the porous nickel plaques.

3.2.3. Current density

A lower level of current density in the impregnation process is always applied (in the range of $5\text{--}100\text{ mA cm}^{-2}$) in order to give a uniform current distribution. A higher total current density may cause nitrate reduction to take place at the surface of the nickel plaque, and thus results in the

obstruction of the pores and non-uniform distribution of the impregnated plaque inside the pores. Nevertheless, a longer impregnation time is required at lower current density and the production cost may be increased. Law and Sapjeta [20] operated at extremely high current densities ($460\text{--}820\text{ mA cm}^{-2}$) for short times, and found that an excessive current density was harmful to the capacity of Fibrex nickel electrodes. Overall, it is easier to apply a high current density to the higher porosity plaque material. The data in Fig. 5 show that the weight gain of the B-type plaque increases with current density to give a constant value of more than 110 mA cm^{-2} . The plaque is impregnated in an aqueous $3.2\text{ M Ni}(\text{NO}_3)_2$ bath (made acidic to a pH of about 3.5) at 60°C for 45 min. For the special ECI process, however, the weight gain decreases when the current density exceeds 90 mA cm^{-2} . Therefore, it is suitable for the B-type porous plaque to use an impregnation system at about 90 mA cm^{-2} for 45 min.

3.2.4. Effect of pH

A change of pH value ($0.9\text{--}4.3$) has no obvious effect on the weight gain of the fibrous nickel plaque. The corrosion of nickel-plate anodes is negligible at 30°C , but increases with a decrease of pH at 60°C . At higher temperatures, it is necessary to apply platinized or other anti-corrosive anodes. The rapid ECI process is less dependent on the pH value. Halpert [15] pointed out the importance of the development of a pH gradient that provides deposition of the hydroxide from the inside of the plaque to the surface in the ECI operation. Studies conducted by Britton [27] at a pH of 3 in $1.5\text{ M Ni}(\text{NO}_3)_2$ for 6–10 h revealed that the deposition rate was lower, but that the adherence of active material was excellent.

3.2.5. Porosity of nickel plaque

Fibrous nickel plaques that consisted of nickel-plated perforated steel with 71–88% average porosity were used in the tests. Porosity is an important determinant of the weight gain of nickel plaques because the highly porous material contains larger amounts of nickel nitrate in the special ECI process and the migration of Ni^{2+} increases with plaque pore volume. The experimental results reveal an increase in the weight gain with increase in plaque porosity. For the 85–95% porosity plaque, however, the ECI operation is more effective after mechanical impregnation with a paste of nickel hydroxide and binding agents [26]. In summary, the special ECI process is more suitable for high-porosity, fibrous nickel plaques because the porous plaques can absorb more nickel nitrate inside the pores.

3.2.6. Impregnation time

When moderate operational conditions are applied, the weight gain of the nickel plaque increases with impregnation time (Fig. 7). The deposition rate depends strongly on the impregnation time at constant current density. The end of impregnation is determined by the decay in the cathode potential and incorrect filling of active material is avoided. The

Table 2
Loading level of B-type nickel plaque with different impregnation times

Special ECI process			Conventional method		
t (min)	w_1^a (g)	ρ_L^b (g cm ⁻³ void)	t (min)	w_1 (g)	ρ_L (g cm ⁻³ void)
9	0.273	0.75	22	0.168	0.46
33	0.469	1.29	33	0.239	0.66
60	0.512	1.41	45	0.325	0.89
83	0.580	1.60	83	0.452	1.24
110	0.584	1.61	120	0.589	1.62

^a w_1 = total weight gain.

^b ρ_L = loading level of active material.

results given in Fig. 7 show that it takes 52 min to conduct the deposition process at 100 mA cm⁻², but the weight gain is lower than that achieved with the special ECI process at 60 mA cm⁻². The special method saves about one-third of the impregnation time to attain the final weight gain (0.58–0.59 g) and gives an increased weight gain of 0.13 g (0.36 g per cm³ void) over the same time period (83 min), comparing with that obtained by the conventional ECI method at 60 mA cm⁻². The loading level at 60 mA cm⁻² is calculated by Eq. (5); the results are listed in Table 2. The loading level of the special ECI process after 33 min is twice that of the general method. Therefore, a saving in impregnation time of 50 min for the same weight gain (0.45 g) can be achieved. If a higher loading level is required, a second impregnation process may be necessary because it is essential to remove ammonium hydroxide, excessive hydroxyl ions and deposition at the plaque surface. For one-step heavy deposition, the ECI process at a lower concentration of Ni(NO₃)₂ and a higher temperature may be a better choice [27]. The accumulation of impurities such as ammonia hydroxide is unavoidable, however, and effective measures are needed for their removal. It is beneficial to use high-porosity nickel plaque to perform the one-step impregnation by means of the special ECI method. In conclusion, the special ECI operation is a rapid impregnation process compared with the conventional ECI method.

3.3. Electrode capacity and utilization of active material

Higher porosity C-, D- and E-type plaques with hollow nickel fibres were used to fabricate the nickel electrodes. The loading level of active material ranged from 1.9 to 2.0 g cm⁻³ void. The theoretical capacity was calculated from the weight gain of the plaque with the assumption that the active material is nickel hydroxide and without considering the addition of cobalt and calcium hydroxide in proportion to the composition of the impregnation solution (Table 1). The specific capacity of the C- and D-type electrodes on the fourth cycle is 141 mAh g⁻¹ at the 0.2C discharge rate. This value exceeds that for state-of-the-art electrodes (viz., 115 mAh g⁻¹) [28]. The data in Table 1 show that the utilization of nickel hydroxide decreases with increase in the amount of hollow fibres. There is also a concomitant increase in electrode thickness.

This is because the larger pore size of the fibrous plaque provides lower electric conductivity between the active material and the substrate surface. After four cycles, the expansion of the plaques demonstrates that the addition of hollow fibres improves the flexibility of the nickel porous plaques (Table 1). Given the higher utilization of the C-type electrode and the lower expansion of the E-type electrode, it is concluded that an electrode with 50% hollow nickel fibres has good electric conductivity, while that with 100% hollow fibres exhibits better anti-swelling performance.

The charge/discharge curves for the C-type electrode on the fourth cycle are shown in Fig. 8. The charge potential does not increase after charging for 5.5 h. The discharge potential is 270–350 mV versus HgO/Hg electrode.

The effect of the discharge rate on the utilization of active material was examined; the results are presented in Fig. 9. All charge operations were conducted at the 0.5C rate for 160 min. The capacity and utilization of both C- and D-type electrodes decrease slightly with increase in the discharge rate. The capacity of the C-type electrode is lower than that of the D-type, but the utilization of active material is higher because the C-type electrode consists of 50% nickel powder and has a small pore-size distribution, that yields an improvement in electric conductivity at different discharge rates. Johnson et al. [29] pointed out that the decrease in utilization is due to the mass-transport impedance through the thick films and to the deficiency of protons within the active material near the reaction sites. When the discharge rate is less than 0.5C, however, the utilization of the C-type electrode is greater than 85%.

Nickel electrodes with high loading levels are essential for cylindrical nickel-metal hydride batteries with high specific energies. The electrode swelling at a high loading level is strongly related to battery cycle life. This is discussed in section 3.4.

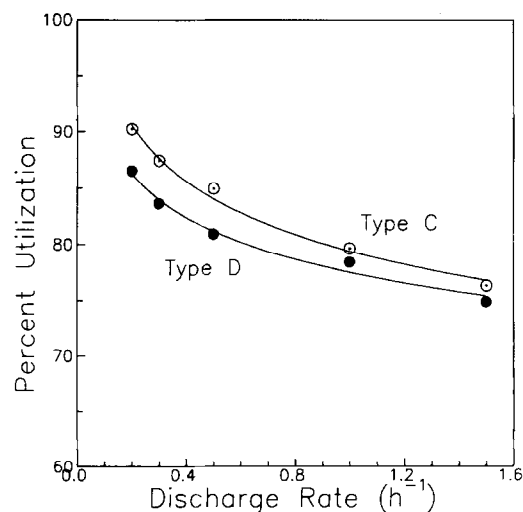


Fig. 9. Percent utilization as function of discharge rate. Charge: 0.5C for 160 min.

3.4. Cycling and swelling tests of fibrous nickel electrodes

Cycling tests were performed (see above) in order to understand the relationship between capacity, utilization and cycle life. The results for C- and D-type electrodes are given in Figs. 10 to 12. The electrode capacity and utilization are relatively constant. The 11th, 12th and 13th cycles were performed at discharge rates of 0.5C, 1.0C and 1.5C, respectively. It is found that the utilization decreases to some extent on the 14th cycle. Therefore, a high discharge rate is somewhat harmful to the capacity of thin nickel electrodes. The damage to the fibrous electrode results from a drop in the density of active material that is brought about by the relatively larger pore size and the swelling in thickness. The latter is caused by the volume changes that accompany the different crystal products. Porous plaques, initially loaded with active material, are found to have 5–8% expansion for C- and D-type electrodes (Fig. 12). When the C-type electrode is subjected to more than six cycles, the thick dimension of the porous plaque exhibited 18% swelling. Electrode expansion will lead to a degradation in the capacity of porous nickel electrodes. Oshitani and co-workers [30,31] suggested that certain amounts of $\text{Co}(\text{OH})_2$ and $\text{Cd}(\text{OH})_2$ added to $\text{Ni}(\text{OH})_2$ crystals will prevent the formation of a higher oxide, $\gamma\text{-Ni}(\text{OH})_2$ so that the degree of swelling is restricted to a lower level ($\sim 10\%$) with a loading level of 1.7 g cm^{-3} over a 100-cycle operation. It should be noted, however, that cadmium additive is harmful to the environment. Hence, it is necessary to search for more appropriate additives. From the above results, it is found that the addition of fibre can also decrease the degree of electrode expansion because the use of hollow fibre can increase both the flexibility and the effective void volume of the porous plaques. Furthermore, it is possible to fill the nickel hydroxide into the inner pores of the hollow fibres.

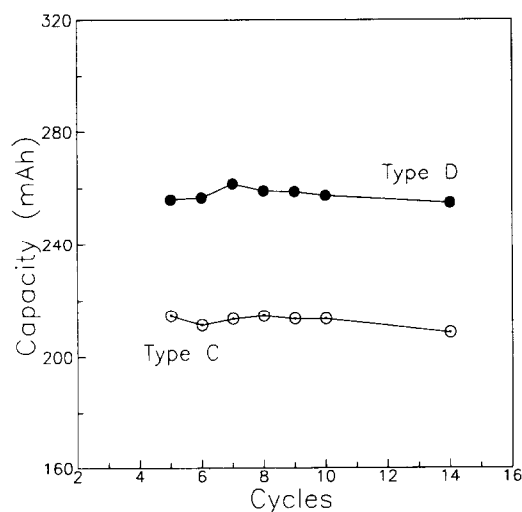


Fig. 10. Plots of capacity vs. cycle number. Charge: 0.5C for 160 min; discharge: 0.3C to 0.0 V vs. HgO/Hg electrode.

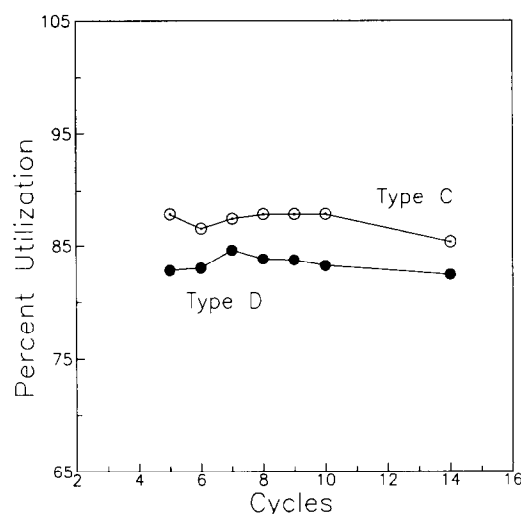


Fig. 11. Percent utilization as function of cycle number. Charge: 0.5C for 160 min; discharge 0.3C to 0.0 V vs. HgO/Hg electrode.

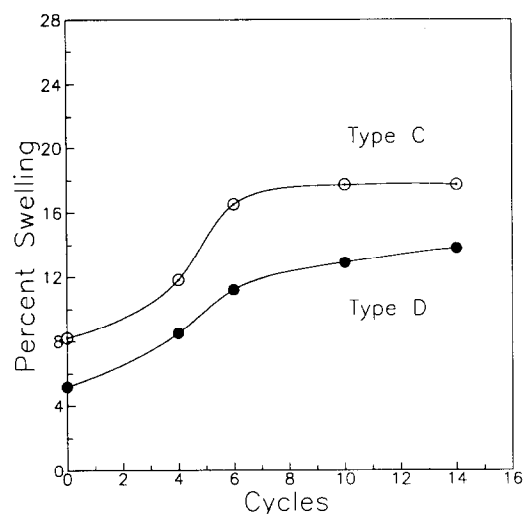


Fig. 12. Electrode swelling as function of cycle number. Charge: 0.5C for 160 min; discharge 0.3C to 0.0 V vs. HgO/Hg electrode.

4. Conclusions

The use of hollow nickel fibres increases the porosity of nickel plaques, while the loading weight of active material increases with the subsequent improvement in plaque porosity. Test results demonstrate the sensitivity of the weight gain of the porous nickel plaques to most of the parameters involved in the ECI process. The impregnation conditions are important in the preparation of porous nickel plaque and the required loading level. Filling the porous plaque in advance with nickel nitrate of high concentration can accelerate the ECI process.

Nickel electrodes using these types of fibrous plaques that have unique small pore size and high porosity, as well as excellent elasticity, will find wide employment in high-power applications such as commercial aircraft and electric vehicles. The use of porous plaques made from hollow nickel fibres

increases the plaque flexibility and prevents large expansion of the fibrous plaque during cycling operations. The C-type electrode has a lower discharge capacity but a higher utilization of nickel hydroxide than the D-type one. The specific capacity of both C- and D-type electrodes reaches 141 mAh g^{-1} and is 23% higher than state-of-the-art equivalents. Further investigations of such electrodes for high specific capacity nickel–metal hydride batteries should be directed towards identifying a cheap and non-hazardous additive that will prevent excessive expansion of the electrode and will improve the utilization of active material.

Acknowledgements

The authors thank Dr C.F. Yang for reading the manuscript and providing stimulating discussions. Thanks are also due to Associate Professor B.H. Li for his enthusiasm and collaboration in getting this work started. Finally, the authors are grateful to Mr. W.C. Lu for providing the perforated iron foils and to Mr. Y.J. Yan for obtaining the electron micrographs.

References

- [1] F. Haschka, G. Benzure-Utmossy and M. Anderman, *Proc. 34th Int. Power Sources Symp., Institute of Electric and Electronic Engineers, New York, USA, 1990*, pp. 286–294.
- [2] G. Bronoel, N. Tassin, T. Potier, S. Bessf and R. Rouget, *Proc. Eur. Space Power Conf., ESA-SP-320, Florence, Italy, 1991*, p. 293.
- [3] W.A. Ferrando, *Proc. 35th Int. Power Sources Symp., Cherry Hill, NJ, USA, 1992*, p. 141.
- [4] M. Anderman and E. McHenry, *Proc. 35th Int. Power Sources Symp., Cherry Hill, NJ, USA, 1992*, p. 149.
- [5] D.L. Britton, *NASA-TM-100958* (1988).
- [6] D.L. Britton, *NASA-TM-105638* (1992).
- [7] J.F. Joyce, *US Patent No. 4 298 393* (1981).
- [8] S.L. Colucci, *US Patent No. 4 312 670* (1982).
- [9] B. Bugnet and D. Doniat, *Proc. 31st Power Sources Symp., The Electrochemical Society, Pennington, NJ, USA, 1984*, p. 171.
- [10] P. Peter, *Proc. 31st Power Sources Symp., The Electrochemical Society, Pennington, NJ, USA, 1984*, p. 195.
- [11] F. Haschka and D. Schliek, *Proc. 32nd Int. Power Sources Symp., The Electrochemical Society, Pennington, NJ, USA, 1986*, p. 420.
- [12] D.J. Zhang, S.M. Lo and Z.K. Wang, *Chin. Patent No. 1 034 880* (1989).
- [13] E.J. McHenry, *Electrochem. Technol.*, **5** (1967) 275.
- [14] R.L. Beauchamp, *US Patent No. 3 653 967* (1972).
- [15] G. Halpert, *J. Power Sources*, **12** (1984) 177.
- [16] L. Kandler, *Br. Patent No. 917 291* (1963).
- [17] E. Hausler, in *Power Sources*, D.H. Collins (ed.), Pergamon, Oxford, 1966, p. 287.
- [18] T. Takamura, T. Shirogam and T. Nakamura, *Denki Kagaku*, **42** (1974) 582.
- [19] K.N. Patric and E.W. Schneider, *J. Electrochem. Soc.*, **133** (1986) 17.
- [20] H.H. Law and J. Sapjeta, *J. Electrochem. Soc.*, **135** (1988) 2418.
- [21] M. Paszkiewicz, *J. Applied Electrochem.*, **11** (1981) 443.
- [22] K.C. Ho and J. Jorne, *AIChE Symp. Ser.*, **83** (1987) 87.
- [23] K.C. Ho and J. Jorne, *J. Electrochem. Soc.*, **137** (1990) 149.
- [24] F. Portemer, A. Delahaye-Vidal and M. Figlarz, *J. Electrochem. Soc.*, **139** (1992) 671.
- [25] M.D. Scherer, *Proc. 17th Intersociety Energy Conversion Engineering Conf., Los Angeles, CA, USA, 1982*, p. 701.
- [26] S.G. Ramos and M. Luisa, *Eur. Patent Applic. 0 547 998* (1992).
- [27] D.L. Britton, *Proc. 34th Int. Power Sources Symp., Institute of Electric and Electronic Engineers, New York, USA, 1990*, p. 235.
- [28] H.S. Lim and G.R. Zelter, *J. Power Sources*, **45** (1993) 195.
- [29] B.A. Johnson, R.E. Ferro, G.M. Swain and B.J. Tatarchuk, *J. Power Sources*, **47** (1994) 251.
- [30] M. Oshitani, Y. Sakaki and K. Takashima, *J. Power Sources*, **12** (1984) 219.
- [31] M. Oshitani, T. Takayama, K. Takashima and S. Tsuji, *J. Appl. Electrochem.*, **16** (1986) 403.